Available online at www.sciencedirect.com

ScienceDirect

IFAC PapersOnLine 52-8 (2019) 154–161

IFAC Papers Online CONFERENCE PAPER ARCHIVE

Vehicle Dynamics State Estimation and Localization for High Performance Race Cars ⋆

Alexander Wischnewski * **Tim Stahl** ** **Johannes Betz** *** **Boris Lohmann** ****

* *Chair of Automatic Control, Department of Mechanical Engineering, Technical University of Munich, Germany (e-mail: alexander.wischnewski@tum.de)*

** *Chair of Automotive Technology, Department of Mechanical Engineering, Technical University of Munich, Germany (e-mail: stahl@ftm.mw.tum.de)*

*** *Chair of Automotive Technology, Department of Mechanical Engineering, Technical University of Munich, Germany (e-mail: betz@ftm.mw.tum.de)*

**** *Chair of Automatic Control, Department of Mechanical Engineering, Technical University of Munich, Germany (e-mail: lohmann@tum.de)*

Abstract: Autonomous driving requires accurate information about the vehicle pose and motion state in order to achieve precise tracking of the planned trajectory. In this paper we propose a robust architecture to localize a high performance race car and show experimental results with speeds up to 150 km h^{-1} and utilizing approximately 80% of the available friction level. The concept has been applied using the development vehicle *DevBot* taking part in the Roborace competition. To achieve robust and reliable performance, we use two independent localization pipelines, one based on GPS and one on LIDARs. We propose to fuse them via a Kalman Filter based on a purely kinematic model and show, that it can outperform a high fidelity model under realistic race conditions. An outstanding property of this concept is that it does not depend on any of the vehicles parameter and is therefore robust to varying tire and track conditions. Further we present an adaption method for the measurement covariances based on the track layout. This allows to combine the strengths of each localization method.

Keywords: State Estimation, Sensor Fusion, Robust Performance, Autonomous Vehicles, Kalman Filters

1. INTRODUCTION

Racing has been driving the advance of automotive technology for decades. The combination of high-performance vehicles and people's enthusiasm allows to identify potential research directions and shortcomings of already available technology, since the vehicle's limits are pushed in order to minimize the achieved lap times.

A research group of the TUM is taking part in the Roborace Competition, which aims at being the first ever full size racing series for autonomous vehicles (Betz et al. (2018)). All competitors use identical cars which are equipped with several vehicle dynamics and environment perception sensors. The experimental setup is a full-sized race car called *DevBot* (see Figure 1). The computations are carried out on a Speedgoat Mobile Target Machine and a NVIDIA Drive PX2. Details on the vehicle can be found in Betz et al. (2018). The TUM software stack reached a near-human performance level, was able to drive

Fig. 1. Research Plattform - *DevBot*

⋆ Research was supported by the basic research fund of the Institute of Automotive Technology of the Technical University of Munich.

10.1016/j.ifacol.2019.08.064

at 150 km h^{-1} and utilized the friction circle up to 80% of the physical limit.

In this paper, we present a Kalman Filter based algorithm to fuse the independent localization pipelines for GPS and LIDAR with an odometry based on vehicle dynamics sensors. The motorsports application demands that the full range of vehicle dynamics, changing track conditions and setup changes are covered without quality degradation. At the same time, it is crucial that the system is robust and easy to tune since testing time is limited and costly. In the following, we show that filter models based purely on kinematic equations can outperform a high fidelity vehicle model in terms of performance and robustness. Furthermore, we apply several modifications to the standard Kalman Filter algorithm to maximize the performance for the given race track scenario.

The remaining paper is organized as follows: Section 2 reviews the state of the art of autonomous driving state estimation and localization, while Section 3 recapitulates the theoretical fundamentals of the applied concept. Section 4 outlines the system architecture, Section 5 goes into detail regarding the state estimation concept used and Section 6 presents experimental data from the real vehicle.

2. RELATED WORK

The state estimation applications in vehicle technology can be roughly separated into two tasks:

- Estimation of the vehicle dynamic state (longitudinal and lateral velocity, yaw rate)
- Localization of the vehicle (position and orientation, also known as pose)

The former has been in the focus of research for several decades. A comparison of the results can be found in Guo et al. (2018). In general, one can divide the models used into three types: detailed vehicle models with tire force characteristics, slip-free constant velocity kinematic models and kinematic models also considering accelerations. The most common representative of the first category is the pure lateral single track model (Farrelly and Wellstead (1996); Haiyan and Hong (2006)). The longitudinal velocity is considered as a parameter but not estimated within a joint framework. Zhao et al. (2011) use a three degrees of freedom model to overcome this drawback. Even more complex models were applied but they are usually tailored to the specific use case and lack good generalization properties. Examples are the extension to more degrees of freedom (Wenzel et al. (2006)), use of suspension parameter knowledge (Antonov et al. (2011)) or the addition of parameter estimations (Wielitzka et al. (2014)). In contrast, slip-free constant velocity kinematic models provide higher robustness with respect to parameter uncertainty and are easier to tune since they require only the effective front axle steering angle (Kang et al. (2014)). They are mostly used within robotics to improve pose accuracy (Bonnifait et al. (2001)), rather than in vehicle dynamics related applications since they lack accuracy under significant accelerations. The third approach relies on the use of first principles modelling by the use of kinematic equations (Du and Li (2014); Farrelly and Wellstead (1996)). Instead of modelling the kinematic relations of the vehicle based on the steering angle, they rely on the measured lateral and longitudinal acceleration as the system inputs. This technique is also known as Kinematic Kalman Filter (KKF) (Jeon (2010)). Although it does not consider potentially available detailed knowledge about the model it is considered to be robust to parameter variations.

Following the trend towards autonomous driving, the focus is nowadays shifting towards the localization task and the necessary system architectures. While automotive applications have been concentrating on GPS at first, reliability issues posed the need for more robust localization methods. The progress already made in the robotics community led to the applications of probabilistic methods based on visual sensors like LIDARs and cameras. Although the former is the most common and mature framework (Thrun et al. (2005); Cadena et al. (2016)), algorithms which utilize cameras are emerging recently (Usenko et al. (2015); Mur-Artal et al. (2015)). The strengths and weaknesses of different environment perception sensors are discussed in Kuutti et al. (2018). The LIDAR measurements give direct information about the environment and object distances, which can be used for mapping and localization directly. In contrast, camera-based methods require complex post-processing steps to generate map data.

Several authors propose to increase localization performance by fusing different sensor sources within a single algorithm (Trehard et al. (2015); Suhr et al. (2017)). However, we found that this approach leads to difficulties during practical realization as the algorithm is a single point of failure in the system design, and it is hard to implement online diagnosis and reconfiguration possibilities. Bresson et al. (2016) and Jang et al. (2015) propose ideas for overcoming this limitation using a decision method to switch between different localization algorithms. The main drawback of this concept is that it does not combine all available information with respect to the corresponding characteristics under normal operating conditions.

The contribution of the paper is threefold: First, we propose a highly modular sensor fusion framework based on parallel localization pipelines and vehicle sensors using a Kalman Filter. Second, we show that a simple point mass model is sufficient and can even outperform a more sophisticated model for the full speed and nonlinear tire range based on data gathered with a high performance race car. Third, we introduce a covariance adaption for each localization pipeline based on previously available map data.

3. METHODOLOGY

In this section, we present the vehicle dynamics models used later for the design of the state estimator and the theoretical fundamentals of Kalman Filter based sensor fusion and LIDAR based localization.

3.1 Vehicle dynamics

Sensor fusion requires that the signals are related to each other using a dynamic system model. Due to its good trade-off between complexity and accuracy (Milliken and Milliken (1996)), even for operating points within the

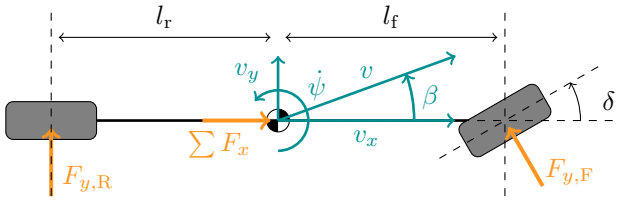

Fig. 2. Nonlinear single track model

nonlinear tire range, the nonlinear single track model is widely applied for control and estimation purposes once the vehicle operates near the handling limit.

The vehicle velocity dynamics (Figure 2) are formulated using the state variables longitudinal v_x and lateral velocity v_y in vehicle coordinates and the yaw rate $\dot{\psi}$. Following first principles modelling using the vehicle mass m, the vehicle inertia J, the longitudinal forces F_x, the lateral forces F_y and the torques T resulting from them, the corresponding differential equations are

$$\dot{v}_x = \frac{1}{m}\sum F_x + \dot{\psi} v_y \ , \tag{1a}$$

$$\dot{v}_y = \frac{1}{m}\sum F_y - \dot{\psi} v_x \ , \text{ and} \tag{1b}$$

$$\ddot{\psi} = \frac{1}{J}\sum T. \tag{1c}$$

Using the lateral tire force characteristics for the front $F_{y,\mathrm{F}}(\alpha_\mathrm{F})$ and the rear axle $F_{y,\mathrm{R}}(\alpha_\mathrm{R})$ depending on the tire side slip angles α_F and α_R, the full nonlinear single track model can be formulated as

$$\dot{v}_x = \frac{1}{m}\left[F_x - F_{y,\mathrm{F}}(\alpha_\mathrm{F})\sin(\delta)\right] + \dot{\psi} v_y \ , \tag{2a}$$

$$\dot{v}_y = \frac{1}{m}\left[F_{y,\mathrm{F}}(\alpha_\mathrm{F})\cos(\delta) + F_{y,\mathrm{R}}(\alpha_\mathrm{R})\right] - \dot{\psi} v_x \ , \text{ and} \tag{2b}$$

$$\ddot{\psi} = \frac{1}{J}\left[F_{y,\mathrm{F}}(\alpha_\mathrm{F})\cos(\delta) l_\mathrm{f} - F_{y,\mathrm{R}}(\alpha_\mathrm{R}) l_\mathrm{r}\right]. \tag{2c}$$

Details on the derivation can be found in Milliken and Milliken (1996). We represent the lateral tire force characteristics by a basic four coefficient Pacjeka model as described in Pacejka (2006).

The autonomous driving task requires the tracking of trajectories in inertial coordinates. The relationship between the vehicle dynamic states and the movement in global coordinate frame can be described via

$$\dot{q}_1 = \cos(\psi) v_x - \sin(\psi) v_y \text{ and} \tag{3a}$$

$$\dot{q}_2 = \sin(\psi) v_x + \cos(\psi) v_y, \tag{3b}$$

with the east coordinate q_1, the north coordinate q_2 and the vehicle heading ψ obtained by integration of the yaw rate $\dot{\psi}$.

3.2 State estimation

In general, the stochastic framework leads to intuitive implementations of state estimation algorithms. Its most common form is the Kalman Filter, which can be used to construct an estimator for linear discrete time dynamic systems of the form

$$x(k+1) = Ax(k) + Bu(k) + w(k) \tag{4a}$$

$$y(k) = Cx(k) + v(k), \tag{4b}$$

with the state vector $x \in \mathbb{R}^n$, the input vector $u \in \mathbb{R}^p$ and the measurement vector $y \in \mathbb{R}^m$. The matrices A, B and C are defined to have appropriate dimensions. The process noise $w(k) \in \mathbb{R}^n$ and the measurement noise $v(k) \in \mathbb{R}^m$ are assumed to have zero mean and to be normally distributed and uncorrelated over time (white noise). Their covariance matrices are denoted with Q for the process noise and R for the measurement noise.

The following overview is based upon the derivations given in Gelb et al. (1974) and Simon (2006). At the core of the Kalman filter algorithm is the propagation of mean and covariance of the state estimate. We will denote the maximum likelihood estimate, which is identical to the mean value due to the gaussian properties of the underlying random variables, by $\hat{x}$.

Prediction Based on the information up to time k we obtain the best possible estimate for time $k+1$ by applying the system model equation. We denote this by

$$\hat{x}(k+1|k) = A\hat{x}(k|k) + Bu(k), \tag{5}$$

where $(k+1|k)$ denotes the prediction for the time instance $k+1$ based on the information available up to the time instance k. Accordingly, $(k|k)$ describes the corrected state estimate based on the information available at time k. Using the definition of covariance and the underyling random process (4), we obtain the covariance of the prediction

$$\Sigma_{xx}(k+1|k) = A\Sigma_{xx}(k|k)A^T + Q, \tag{6}$$

where Q describes the process covariance for a one-step update.

Correction The second ingredient of the algorithm is to update the prediction based on the given measurements. This forms the stabilizing mechanism of the estimator. If the system is observable for the pair (C, A), it also guarantees that it converges to the true value. Note that this is only holds under the assumption of zero-mean measurement noise. This fact can be of significant practical relevance due to sensor calibration errors. Based on the prediction step, the measurement residual

$$r(k+1) = y_\mathrm{m}(k+1) - C\hat{x}(k+1|k) \tag{7}$$

is calculated. We denote the actual measured value by y_m. Based on the statistical properties of the system, one can calculate the Kalman Gain matrix

$$K = \Sigma_{xx}(k+1|k)C^T(R + C\Sigma_{xx}(k+1|k)C^T)^{-1}, \tag{8}$$

such that the overall estimator is optimal in terms of minimum variance. It remains to update the predicted state estimate

$$\hat{x}(k+1|k+1) = \hat{x}(k+1|k) + Kr(k+1). \tag{9}$$

Due to the nonlinearity of the state equations (2) and (3), the presented algorithm cannot be applied directly. Several modifications are available in the literature (Simon (2006)); most widely known the Extended Kalman Filter (EKF). It relies either on analytic or numeric linearization. The algorithm itself is conceptually similar to the alternating process between prediction and correction described in this section. This follows from the fact that, assuming that they are exact at the given time instant, the equations can be rewritten using time-varying matrices. It follows, that it is a necessary condition for stable operation that the estimate is properly initialized and stays sufficiently close to the real value.

Table 1. *DevBot* Sensor Configuration

Sensor	Type
Accelerometer	McLaren Applied Technologies 3-axis
Gyroscope	McLaren Applied Technologies 1-axis
Wheelspeeds	McLaren Applied Technologies
Optical speed	Kistler Correvit SF-II
GPS	OXTS 4002
LIDAR	Ibeo Scala B2

3.3 LIDAR Localization

The localization software utilizes the Adaptive Monte Carlo Localization (AMCL) algorithm presented in Thrun et al. (2005) for localization. It is conceptually similar to the Kalman Filter, but it implements a Particle Filter, which is based on a sample based representation of the underlying stochastic distribution. Based on the point clouds from the LIDAR sensors, the vehicle corrects its position by comparing the measurements to the fixed map. To increase the performance in featureless spaces, such as long straights, a motion model is used. The algorithm assumes the track map to be constant, which improves robustness and computational efficiency compared to a SLAM algorithm in a fixed environment. The map is obtained in advance of the race during a slow manual driving lap. Details of the applied concept are presented in Stahl et al. (2018).

4. SYSTEM ARCHITECTURE

The sensor fusion task for the localization and vehicle dynamics of the *DevBot* concentrates on the following points:

- Providing a well-structured framework to increase localization accuracy by combining different data sources
- Reducing the measurement noise (especially of longitudinal and lateral velocities) to improve the control performance
- Handling the asynchronous and delayed timing characteristics of the LIDAR based localization

The relevant sensors of the *DevBot* are listed in Table 1. To achieve a modular design, it was important to keep the localization pipelines itself indepenent of each other. Each of them outputs a pose estimate which is then finally fused with the odometry obtained from the IMU and the optical speed sensor as depicted in Figure 3. The latter is preferred to the wheelspeeds as they cannot measure the slip-free velocity in an all-wheel drive powertrain. The odometry required by the LIDAR localization is purely based on optical speed sensor measurements and is not prefused with any other sensor.

The components of the system are distributed onto both available computation units. The Drive PX2 is better suited for LIDAR data processing due to the large data amounts and longer processing times. The real-time capabilitites of the Speedgoat allow for incorporating high-frequency sensor updates and achieving a smooth interpolation between the localization updates. This improves

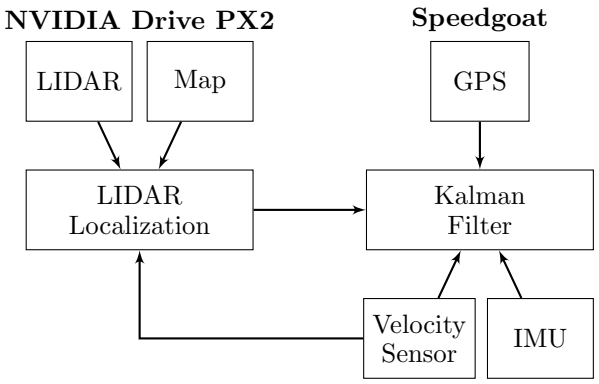

Fig. 3. State estimation architecture with both processing units. The communciation between these two is implemented via UDP.

the control accuracy and enables high frequency feedback control.

5. KALMAN FILTER DESIGN

5.1 Model Choice

Comparing the state estimation and filtering approaches presented above, one can observe that the kinematic and the dynamic models are both exact in terms of mean value prediction capabilities (compare (1) and (2)). In practical applications, the estimation performance is highly dependent on the match between the physical system and the differential equation model. This requires that all parameters used in the model must be known exactly or must be estimated during operation. The latter requires precise sensors and slows the transient response times of the estimation. In contrast, the kinematic approach uses measured acceleration values instead of any model parameter to calculate the prediction. This is beneficial in the racing application, since the model parameters will never be exact on different tracks or varying weather conditions. It thus promises a consistent and predictable system performance.

We will compare both approaches in the following, using a nonlinear single track model (STM) and a kinematic point-mass model with acceleration measurements (PM) as inputs. GPS and LIDAR based localization are unlikely to exhibit random noise but can show significant systematic measurement error. In the case of GPS, this can be caused by undesired reflections of the signals from the environment. In case of LIDAR, this can be caused by mapping errors. Since the resulting estimation errors increase significantly with non-zero mean measurement errors, this could have negative impact on the precision of the velocity state estimates. To overcome these drawbacks, additionally a modified version of the point-mass model (MPM) is proposed. It uses a cascaded Kalman Filter with separated velocity and position dynamics. The former uses the IMU measurements as system inputs and (1) as a system model, while the latter takes the fused velocities and the yaw rate as inputs and uses (3) as the underlying system model. This separation prevents the measurement update triggered by the localization from affecting the velocity estimates. However, this setup strictly requires that the optical wheelspeed sensor is available since the

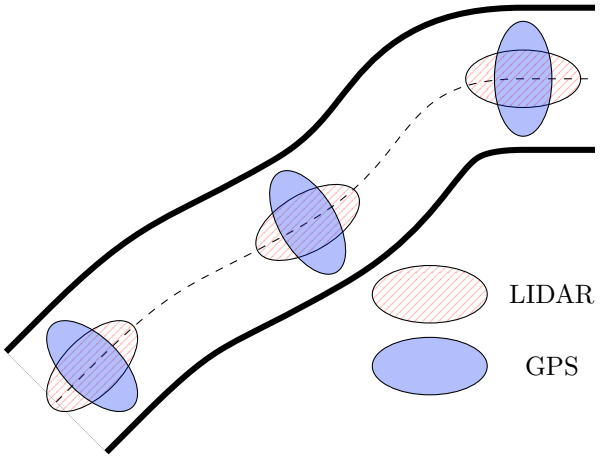

Fig. 4. Visualization of the transformation applied to the covariance matrices of the localization measurements. The resulting uncertainty ellipses are oriented along the track and depicted for three different vehicle positions. The LIDAR covariance in the lateral direction is smaller than the GPS covariance. Therefore, the LIDAR is weighted more strongly in lateral direction. the GPS is weighted more strongly in longitudinal direction.

velocity subsystem becomes otherwise unobservable. Furthermore, it should be noted that both point-mass models are not capable of filtering the yaw rate as no derivative information can be obtained from the current sensor setup.

5.2 Covariance Adaption

Even though the GPS platform used is highly accurate under normal conditions, its absolute performance may be unsufficient dependending on the environment condition. The LIDAR localization was found to be able to locate the vehicle within 20 cm of lateral deviation. However, it struggles to generate exact longitudinal measurements in featureless spaces such as long straights. A small, but important difference between the two systems is, that the LIDARs are positioning the vehicle relative to its obstacles while the GPS is referring to a global coordinate system. In case there are map errors, the former is more robust since it guarantees that the vehicle will stay within the planned safety margin.

The Kalman Filter approach provides a well-suited tool to incorporate the knowledge we have about the individual sensor accuracy. We assign the task of lateral estimation strongly to the LIDAR sensor, while the GPS is taking care of the longitudinal position as depicted in Figure 4. The measurement covariance matrix for each sensor is rotated according to the track orientation ψ_T by

$$R_\mathrm{loc} = T(\psi_\mathrm{T}) \begin{bmatrix} \sigma_\mathrm{long} & 0 \\ 0 & \sigma_\mathrm{lat} \end{bmatrix} T^\mathrm{T}(\psi_\mathrm{T}) \tag{10}$$

with

$$T(\alpha) = \begin{bmatrix} \cos(\alpha) & -\sin(\alpha) \\ \sin(\alpha) & \cos(\alpha) \end{bmatrix} \tag{11}$$

being the standard rotation matrix.

5.3 Incorporation of Asynchronous Measurements

The Kalman Filter is propagating mean and covariance of its estimates for every step according to the underlying process and measurement model. This allows time-varying models to be easily incorporated through modification of the corresponding equations. The fact that the localization measurements are available asynchronously is therefore addressed by the use of different measurement vectors. Depending on the available measurement signals, it can be written as:

$$y_\mathrm{M} = \begin{cases} \begin{bmatrix} x_\mathrm{G} & y_\mathrm{G} & \psi_\mathrm{G} & v_x & v_y \end{bmatrix}^\mathrm{T}, \\ \text{if only GPS available} \\ \begin{bmatrix} x_\mathrm{L} & y_\mathrm{L} & \psi_\mathrm{L} & v_x & v_y \end{bmatrix}^\mathrm{T}, \\ \text{if only LIDAR available} \\ \begin{bmatrix} x_\mathrm{G} & y_\mathrm{G} & \psi_\mathrm{G} & x_\mathrm{L} & y_\mathrm{L} & \psi_\mathrm{L} & v_x & v_y \end{bmatrix}^\mathrm{T}, \\ \text{if LIDAR \& GPS available} \\ \begin{bmatrix} v_x & v_y \end{bmatrix}^\mathrm{T}, \text{ else} \end{cases} \tag{12}$$

5.4 Time Delay Compensation

Since the processing of LIDAR measurements takes some time, it was found that there is a significant delay of approximately 40 ms between the LIDAR and GPS position signal. This can be compensated for by obtaining an odometry estimate from the measured longitudinal and lateral velocities and the yaw rate. It is calculated by forward integration of (3). The correction itself is then taken from

$$q_{1,\mathrm{comp}}(t) = q_{1,\mathrm{odom}}(t) - q_{1,\mathrm{odom}}(t - 40\,\mathrm{ms}) \tag{13a}$$
$$q_{2,\mathrm{comp}}(t) = q_{2,\mathrm{odom}}(t) - q_{2,\mathrm{odom}}(t - 40\,\mathrm{ms}) \tag{13b}$$
$$\psi_\mathrm{comp}(t) = \psi_\mathrm{odom}(t) - \psi_\mathrm{odom}(t - 40\,\mathrm{ms}). \tag{13c}$$

In fact, the compensation values measure the difference between the purely forward integrated vehicle poses at the actual time and the time when the LIDAR measurement is captured. $q_{1,\mathrm{comp}}(t)$, $q_{2,\mathrm{comp}}(t)$ and $\psi_\mathrm{comp}(t)$ is an estimate of the vehicle motion between these two points in time.

6. EXPERIMENTAL RESULTS

The filter structure proposed in this paper was tested in the full-size race car *DevBot* on an airfield. The data was collected in several runs with speeds up to 150 km h^{-1} and acceleration up to 8.5 m s^{-2} in longitudinal and lateral direction for the trajectory planning algorithm. This corresponds roughly to 80 % of the maximum achievable acceleration in steady state cornering. In the following we analyze a 20 s segment, consisting of high speed driving as well as cornering situations. The evaluation is strongly based on the measurement residuals as no ground truth data is available. The residuals capture the mismatch between the model-based prediction and the measured value. A precise definition can be found in (7). The point-mass models utilize an Extended Kalman Filter with analytic derivatives for linearization. The STM is implemented based on an Extended Kalman Filter with numerically obtained derivatives since they cannot be derived trivially as in the point-mass case. Both are discretized using an Euler-Forward scheme with a sample rate of 4 ms.

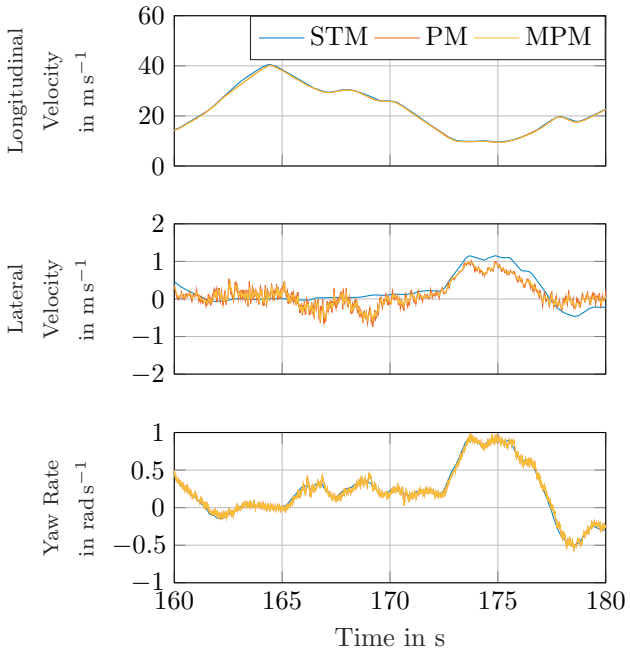

Fig. 5. Estimates of the dynamic states of the vehicle using different process models. The single track model (STM) shows significant offset with respect to point mass models, while the point mass model (PM) and the modified point mass (MPM) model exhibit stronger noise. This effect can be related to the stronger model assumptions of the STM.

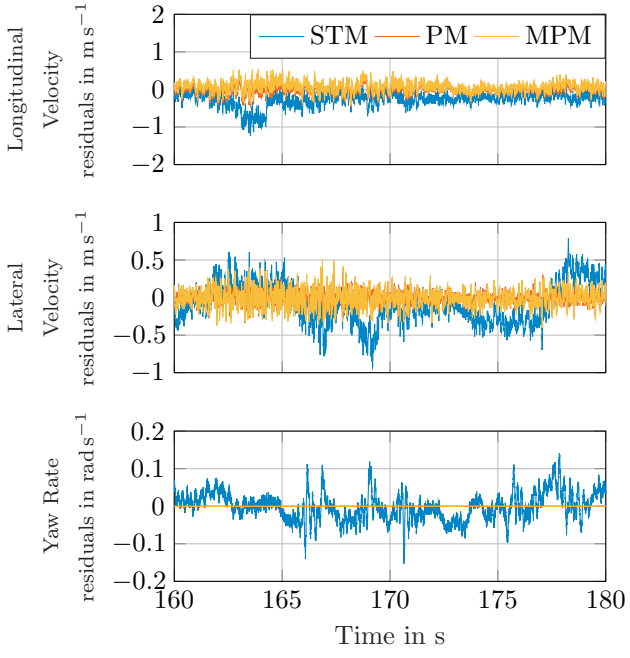

Fig. 6. Residuals of the dynamic state measurements of the vehicle using all available sensors. The single track model (STM) produces non-zero mean residuals which is an indicator for system/model mismatch. In comparison, the point mass model (PM) and the modified point mass model (MPM) perform better. The yaw rate is only estimated by the (STM).

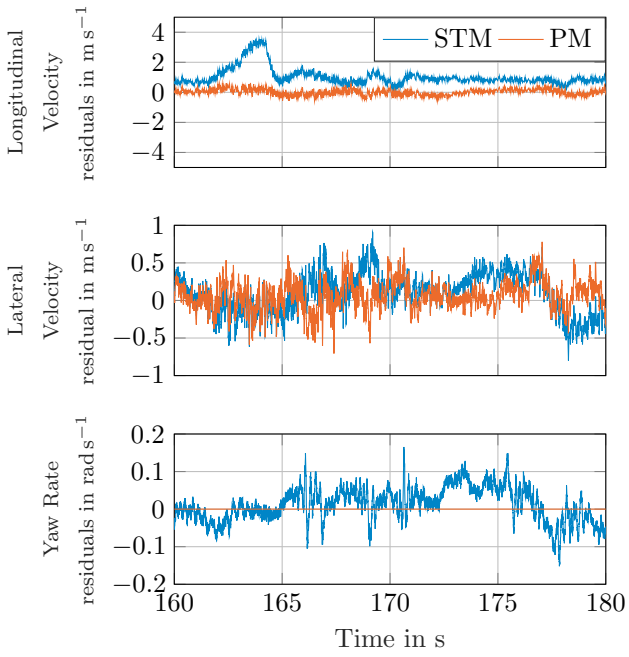

Fig. 7. Residuals of the dynamic state measurements of the vehicle with the optical velocity sensor not available. Therefore the modified point mass model suffers from a loss of observability and could not be compared. The point-mass model significantly outperforms the nonlinear vehicle model in this setting.

We will discuss two cases: All sensors are available in the first case. Figure 5 shows the state estimation performance for all measurements available of the three different structures discussed before. While the PM and the cascaded version MPM show comparable performance, the high-fidelity STM shows better noise rejection properties but also a systematic estimation offset. This is undermined by the residuals depicted in Figure 6, which are non-zero mean for all states estimates of the STM.

In the second case, we assume the optical speed sensor to be unavailable. This case is interesting because the optical velocity sensor is not redundant in our current setup and is also seldom available in other vehicle configurations. The cascaded point mass filter could not be utilized in this case, since the design system becomes unobservable. Figure 7 depicts the residuals of the other models. Note that the velocity residuals were not used for estimation purposes, rather only for validation. In this scenario, the point mass model significantly outperforms the nonlinear single track model, especially for the longitudinal velocity. This mismatch results from the fact that the drivetrain model quality is not sufficient at high speeds. However, the LIDAR odometry is still provided by the optical velocity sensor in this setup. This could be replaced by an odometry based on wheelspeed and IMU sensors to achieve at least a descent prediction quality.

As the last evaluation step, the residuals of the GPS and the LIDAR based position measurement are depicted in Figure 8 for the MPM case with all sensors available. Whereas the residuals of the GPS are small in the longitudinal direction, the LIDAR localization fails to achieve sufficient performance. This is related to systematic errors in

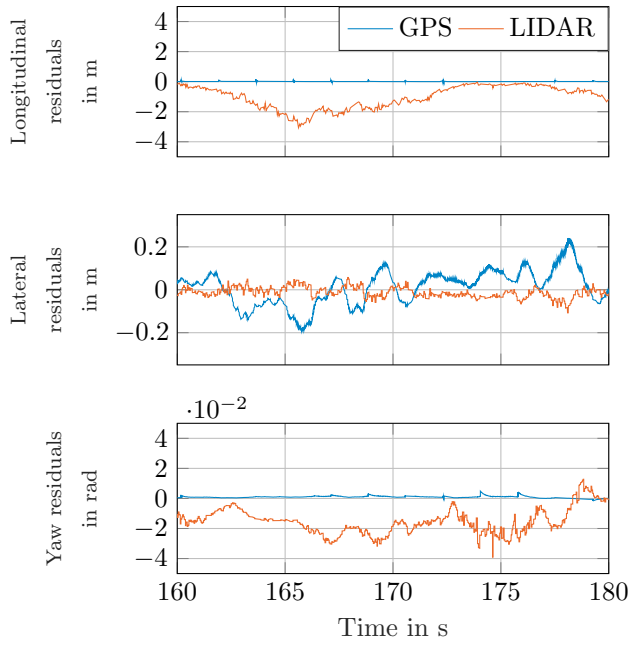

Fig. 8. Residuals of GPS and LIDAR localization measurements of the modified point mass Kalman Filter with optical speed sensor available. The estimate relies heavily on GPS in the longitudinal direction. In the lateral direction the LIDAR measurement is weighted more strongly. Small peaks in GPS residuals are related to a minor timing difference between multiple computation units.

the odometry used combined with the sparse availability of correction features in this direction. The LIDAR is favored over the GPS in lateral direction, which can be seen from the fact that the LIDAR residuals are much smaller than the GPS residuals in the lateral direction. Further, Figure 9 shows the benefical effects of the delay compensation and the covariance adaption. Whereas the former decreases the residuals of the LIDAR position measurement in the longitudinal direction significantly, the latter ensures that the weighting between GPS and the LIDAR is performed as intended. This can be seen from the fact that the GPS longitudinal residuals increase significantly for the case without covariance adaption (NCA). The changes for the lateral localization precision are rather small, but there is an increase in lateral LIDAR residuals for the NCA case. This shows that the lateral LIDAR measurement is weighted more strongly in the case with covariance adaption and that a possible GPS outlier would not disturb the final localization significantly.

7. CONCLUSION

In this paper, we have proposed a novel system architecture for localization and state estimation of autonomous vehicles which proved to be robust and reliable in real-world conditions even in the nonlinear driving range. We evaluated the usability of two purely kinematic models for dynamic state estimation of a race car. Interestingly, they were able to outperform a high-fidelity nonlinear single track model. This is related to the fact that the point-mass model is exact for the whole region of operation of the tires and at high speeds. The main advantage is that

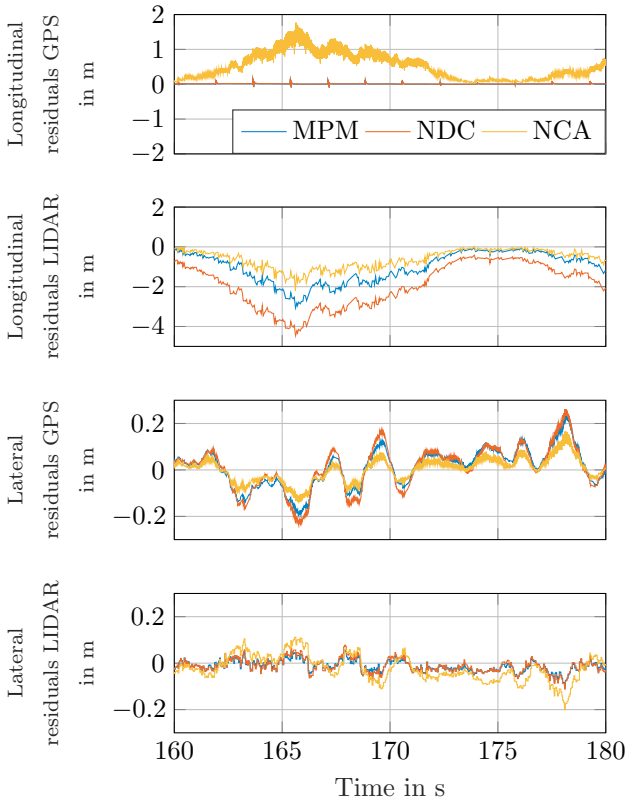

Fig. 9. Residuals of GPS and LIDAR localization measurements of the modified point mass Kalman Filter with different modifications. Whereas the version without the proposed covariance adaption (NCA) suffers from severe GPS residuals in longitudinal direction, the standard version (MPM) weights LIDAR and GPS as expected. This can be seen from small GPS longitudinal and small LIDAR lateral residuals. Without delay compensation (NDC), the longitudinal residuals for the LIDAR increase.

the estimation residuals are zero mean which is important for the design of a high-performance tracking controller. However, this comes at the cost of a slight increase in estimation noise. A positive side-effect is the much lower computational cost and improved robustness due to model simplicity.

Future research will be devoted to automatic reconfiguration of the sensor fusion system in case of sensor failures, e.g. a GPS dropout. The presented sensor fusion implementation itself is capable of handling this already once a failure is known, however the difficulty is the robust detection of those occurences. Furthermore, it is desirable to include camera localization measurements in order to avoid depending on GPS as a secondary localization mechanism at all.

ACKNOWLEDGMENT AND CONTRIBUTIONS

We would like to thank Roborace for the opportunity of evaluating our algorithms on their prototype as well as for their support during the testing sessions and the Berlin event. Further, we thank Madeline Wolz for her support during implementation of the different filter variants and

Johannes Strohm, Mikhail Pak and Leon Sievers for discussions and revision of the paper.

Alexander Wischnewski contributed to the overall system architecture as well as the different estimator designs. Tim Stahl contributed to the design of the visual localization algorithms and the network communication. Johannes Betz and Boris Lohmann contributed equally to the conception of the research project and revised the paper critically for important intellectual content.

REFERENCES

Antonov, S., Fehn, A., and Kugi, A. (2011). Unscented Kalman filter for vehicle state estimation. *Vehicle System Dynamics*, 49(9), 1497–1520.

Betz, J., Wischnewski, A., Heilmeier, A., Nobis, F., Stahl, T., Hermansdorfer, L., Lohmann, B., and Lienkamp, M. (2018). What can we learn from autonomous level-5 Motorsport? *Proceedings of chassis.tech 2018*.

Bonnifait, P., Bouron, P., Crubille, P., and Meizel, D. (2001). Data fusion of four ABS sensors and GPS for an enhanced localization of car-like vehicles. *Proceedings of 2001 IEEE International Conference on Robotics and Automation*, 1597–1602.

Bresson, G., Rahal, M.C., Gruyer, D., Revilloud, M., and Alsayed, Z. (2016). A cooperative fusion architecture for robust localization: Application to autonomous driving. *Proceedings of 2016 IEEE 19th Conference on Intelligent Transportation Systems*, 859–866.

Cadena, C., Carlone, L., Carrillo, H., Latif, Y., Scaramuzza, D., Reid, I., Leonard, J.J., Neira, J., Reid, I., and Leonard, J.J. (2016). Past, Present, and Future of Simultaneous Localization and Mapping: Toward the Robust-Perception Age. *IEEE Transactions on Robotics*, 32(6), 1309–1332.

Du, H. and Li, W. (2014). Kinematics-based parameter-varying observer design for sideslip angle estimation. *Proceedings of 2014 International Conference on Mechatronics and Control*, 2042–2047.

Farrelly, J. and Wellstead, P. (1996). Estimation of Vehicle Lateral Velocity. *Proceedings of the 1996 IEEE International Conference on Control Applications*, 552–557.

Gelb, A., Kasper, J.F., Nash, R.A., Price, C.F., and Sutherland, A.A. (eds.) (1974). *Applied Optimal Estimation*. MIT Press, Cambridge, MA.

Guo, H., Cao, D., Chen, H., Lv, C., Wang, H., and Yang, S. (2018). Vehicle dynamic state estimation: State of the art schemes and perspectives. *IEEE/CAA Journal of Automatica Sinica*, 5(2), 418–431.

Haiyan, Z. and Hong, C. (2006). Estimation of vehicle yaw rate and side slip angle using moving horizon strategy. *Proceedings of 2006 6th World Congress on Intelligent Control and Automation*, 1828–1832.

Jang, S., Ahn, K., Lee, J., and Kang, Y. (2015). A study on integration of particle filter and dead reckoning for efficient localization of automated guided vehicles. In *2015 IEEE International Symposium on Robotics and Intelligent Sensors (IRIS)*, 81–86.

Jeon, S. (2010). State Estimation Based on Kinematic Models Considering Characteristics of Sensors. *Proceedings of the 2010 American Control Conference*, 640–645.

Kang, C.M., Lee, S.H., and Chung, C.C. (2014). Lane estimation using a vehicle kinematic lateral motion model under clothoidal road constraints. *Proceedings of 17th IEEE International Conference on Intelligent Transportation Systems*, 1066–1071.

Kuutti, S., Fallah, S., Katsaros, K., Dianati, M., Mccullough, F., and Mouzakitis, A. (2018). A survey of the state-of-the-art localization techniques and their potentials for autonomous vehicle applications. *IEEE Internet of Things Journal*, 5(2), 829–846.

Milliken, W.F. and Milliken, D.L. (1996). *Race Car Vehicle Dynamics*. Society of Automotive Engineers Inc., Great Britain.

Mur-Artal, R., Montiel, J.M., and Tardos, J.D. (2015). ORB-SLAM: A Versatile and Accurate Monocular SLAM System. *IEEE Transactions on Robotics*, 31(5), 1147–1163.

Pacejka, H. (2006). *Tire and Vehicle Dynamics*. SAE International.

Simon, D. (2006). *Optimal State Estimation: Kalman, H Infinity, and Nonlinear Approaches*. Wiley-Interscience, New York, NY, USA.

Stahl, T., Wischnewski, A., Betz, J., and Lienkamp, M. (2018). Ros-based localization of a race vehicle at high-speed using lidar. In *7th International Conference on Mechatronics and Control Engineering 2018*.

Suhr, J.K., Jang, J., Min, D., and Jung, H.G. (2017). Sensor fusion-based low-cost vehicle localization system for complex urban environments. *IEEE Transactions on Intelligent Transportation Systems*, 18(5), 1078–1086.

Thrun, S., Burgard, W., and Fox, D. (2005). *Probabilistic Robotics (Intelligent Robotics and Autonomous Agents)*. The MIT Press.

Trehard, G., Pollard, E., Bradai, B., and Nashashibi, F. (2015). On line mapping and global positioning for autonomous driving in urban environment based on evidential SLAM. *Proceedings of 2015 IEEE Intelligent Vehicles Symposium*, 814–819.

Usenko, V., Engel, J., Stuckler, J., and Cremers, D. (2015). Reconstructing Street-Scenes in Real-Time from a Driving Car. *Proceedings of International Conference on 3D Vision 2015*, 607–614.

Wenzel, T., Burnham, K., Blundell, M., and Williams, R. (2006). Dual extended Kalman filter for vehicle state and parameter estimation. *Vehicle System Dynamics*, 44(2), 153–171.

Wielitzka, M., Dagen, M., and Ortmaier, T. (2014). State Estimation of Vehicle's Lateral Dynamics using Unscented Kalman Filter. *Proceedings of 53rd IEEE Conference on Decision and Control*, 5015–5020.

Zhao, L.H., Liu, Z.Y., and Chen, H. (2011). Design of a nonlinear observer for vehicle velocity estimation and experiments. *IEEE Transactions on Control Systems Technology*, 19(3), 664–672.